



HAL
open science

Monte Carlo fixed-lag smoothing in state-space models

Anne Cuzol, Etienne Mémin

► **To cite this version:**

Anne Cuzol, Etienne Mémin. Monte Carlo fixed-lag smoothing in state-space models. *Nonlinear Processes in Geophysics*, 2014, 21, pp.633 - 643. 10.5194/npg-21-633-2014 . hal-01074987

HAL Id: hal-01074987

<https://hal.science/hal-01074987>

Submitted on 16 Oct 2014

HAL is a multi-disciplinary open access archive for the deposit and dissemination of scientific research documents, whether they are published or not. The documents may come from teaching and research institutions in France or abroad, or from public or private research centers.

L'archive ouverte pluridisciplinaire **HAL**, est destinée au dépôt et à la diffusion de documents scientifiques de niveau recherche, publiés ou non, émanant des établissements d'enseignement et de recherche français ou étrangers, des laboratoires publics ou privés.

Monte Carlo fixed-lag smoothing in state-space models

Anne Cuzol¹ and Etienne Mémin²

¹Univ. Bretagne-Sud, UMR 6205, LMBA, F-56000 Vannes, France

²INRIA Rennes-Bretagne Atlantique, Rennes, France

Abstract.

This paper presents an algorithm for Monte Carlo fixed-lag smoothing in state-space models defined by a diffusion process observed through noisy discrete-time measurements. Based on a particles approximation of the filtering and smoothing distributions, the method relies on a simulation
5 technique of conditioned diffusions. The proposed sequential smoother can be applied to general non linear and multidimensional models, like the ones used in environmental applications. The smoothing of a turbulent flow in a high-dimensional context is given as a practical example.

1 Introduction

10 The framework of this paper concerns state-space models described by general diffusions of the form:

$$d\mathbf{x}(t) = f(\mathbf{x}(t))dt + \sigma(\mathbf{x}(t))d\mathbf{B}(t), \quad (1)$$

which are partially observed through noisy measurements at discrete times. Such models can describe many dynamical phenomena in environmental sciences, physics, but also in finance or engineering applications. The main motivation of this work concerns environmental applications, where
15 non linearity and high-dimensionality arise. Indeed, environmental models and data describe non linear phenomena over large domains, with high spatial resolution. The continuous dynamical model (1) is defined from *a priori* physical laws, while observations are supplied by sensors (satellite data for instance) and can appear with very low time frequency. As an example, in the application presented in the last part of this paper, the dimension of the state and observations is of the order of
20 many thousands, and the model is described by the non linear Navier-Stokes equation. Filtering

and smoothing in such state-space models aim at coupling model and observations, which is called data assimilation. The goal of the filtering is to estimate the system state distribution knowing past and present observations. This allows for instance to give proper initial conditions to forecast the future state of a system characterizing atmospheric or oceanographic flows. On the other hand, the smoothing aims at estimating the state distribution using past and future observations, and this retrospective state estimation allows to analyze a spatio-temporal phenomenon over a given time period, for climatology studies for instance. Applications of data assimilation are numerous and the interest is growing in environmental sciences with the increase of available data. However, it is still a challenge to develop filtering and smoothing methods that can be used within a general non linear and high-dimensional context.

Monte Carlo sequential methods, contrary to standard Kalman filters, are able to deal with the filtering problem in non linear state-space models. The particle filtering (Del Moral et al., 2001; Doucet et al., 2000) solves the whole filtering equations through Monte Carlo approximations of the state distribution. On the other hand, ensemble Kalman methods (Evensen, 2003) take into account in some way the non linearities in the system, but are based on a Gaussian assumption. For high-dimensional systems, ensemble Kalman methods are preferred in practice to particle filters (Stroud et al., 2010; Van Leeuwen, 2009) since they reach better performance for limited number of particles. In order to keep this advantage while alleviating the Gaussian assumption, both methods are combined in Papadakis et al. (2010), leading to a particle filter that can be applied to high-dimensional systems. We will use this technique for the filtering step in the high-dimensional application presented in Section 5.

The aim of this paper is to propose a new smoothing method. Within the particle filter framework, the smoothing can be computed backward, reweighting past particles using present observations (Briers et al., 2010; Godsill et al., 2004). There is however one main difficulty for continuous models of type (1). As a matter of fact, it is necessary to know the transition density of the process between observation times, which is not available for general diffusions. This transition density can be approximated through Monte Carlo simulations, as proposed by Durham and Gallant (2002) to solve inference problems for diffusion processes. However, these approximations are based on Brownian bridge (or modified versions of it) simulations, that do not take into account the drift part of the model. For non linear and high-dimensional models with a drift term that dominates, such approximations will be inefficient. It is also possible to obtain an unbiased estimate of the transition density (see Beskos et al. (2006)), but this approach is not adapted to a multi-dimensional context. As a matter of fact, the use of this technique in a multivariate setting imposes constraints on the diffusion drift (in particular the drift function has to be of gradient type). In parallel, within the framework of ensemble Kalman methods, Evensen and van Leeuwen (2000) have proposed to estimate backward the smoothing distribution in a recursive way, based on existing filtering trajectories; Stroud et al. (2010) presented and applied an ensemble Kalman smoothing method, relying on a linearization of

the system dynamics.

60 All previously mentioned smoothing methods require to perform specific assumptions or simplifications in order to deal with general non linear models of type (1) in a high-dimensional context. To the best of our knowledge, it remains a challenging problem to develop smoothing methods that can be used in this general setting. In this paper, we deal with this issue sequentially each time a new observation is available, by smoothing the hidden state from this new observation time up to
65 the previous one. This approach, called fixed-lag smoothing, constitutes then a partial answer to the global smoothing problem that would take into account all available observations. Nevertheless, it is reasonable to assume that the distribution of the hidden state depends on future observations through the next observation only, as soon as the time step between measurements is long (which is typically the case in the environmental applications that motivate this work). Under this assumption,
70 a new observation will impact the distribution of the hidden process up to the previous observation only. This point of view justifies the use of a fixed-lag smoothing in our setting as a reasonable approximation of the global smoothing problem.

Such a fixed-lag smoothing may be directly obtained from the particle filtering result, reweighting past trajectories. However, this smoothing will fail in two cases: when the number of particles is
75 too small compared to the size of the system, or when existing trajectories do not correspond to plausible trajectories of the dynamical model. Unfortunately, these two situations have to be faced when smoothing in a high-dimensional state-space model. Firstly, the number of particles has to be reduced for computational reasons. Secondly, particle filters that have been proposed in this high-dimensional context require to correct trajectories towards the observations (Papadakis et al., 2010;
80 Van Leeuwen and Ades, 2013). This implies that filtering states are consistent at observation times, but that filtering trajectories may not be plausible realizations of the underlying physical model. In that case, a smoothing based on existing trajectories will fail. Note that these remarks are not only valid for the fixed-lag smoothing, but also for previously mentioned global techniques relying on existing trajectories. In particular, a genealogical smoothing based on ancestral particle lines
85 (Del Moral, 2004) will be deficient in a high-dimensional setting since many trajectories will share only a few ancestral lines.

In contrast, our method does not rely on existing particles only. It is built on a conditional simulation technique of diffusions proposed by Delyon and Hu (2006) that provides new state trajectories at hidden times between observations. This simulation technique is adapted to a multivariate context
90 where the drift dominates, contrary to techniques based on Brownian bridge sampling (Durham and Gallant, 2002). Moreover, it does not require constraining assumptions for multivariate models, contrary to other techniques based on exact simulation of diffusions (Beskos and Roberts, 2005; Beskos et al., 2006). The proposed smoothing method can then be applied to high-dimensional systems. Finally, it does not require model linearization nor Gaussian hypotheses, and so is able to deal with
95 general non linear models.

The remaining of the paper is organized as follows. Section 2 briefly describes sequential Monte Carlo filtering methods in state-space models, and presents the fixed-lag smoothing problem. Section 3 presents the conditional simulation technique of diffusions of Delyon and Hu (2006), and details the construction of the proposed Monte Carlo estimate of smoothing distributions. The method is then experimented on a one-dimensional example in Section 4. Finally, the method is applied in section 5 to a practical non linear and high-dimensional case, similar to the problems that have to be faced in environmental applications. A discussion is given in Section 6.

2 Monte Carlo filtering and smoothing in state-space models

In this section we recall briefly the particle filtering and smoothing methods for models of type (1), where the hidden state vector $\mathbf{x} \in \mathbb{R}^n$ is observed through the observation vector $\mathbf{y} \in \mathbb{R}^m$ at discrete times $\{t_1, t_2, \dots\}$:

$$\mathbf{y}(t_k) = g(\mathbf{x}(t_k)) + \gamma_{t_k}. \quad (2)$$

The drift function f and observation operator g can be non linear. The dynamical model uncertainty is described by a n -dimensional Brownian motion with covariance $\Sigma = \sigma(\mathbf{x}(t))\sigma(\mathbf{x}(t))^T$. The functions f , g and σ are assumed to be known, as well as the law of the observation noise γ_{t_k} .

In particular, we present the standard particle filter and the Weighted Ensemble Kalman filter, that can be used to face the filtering problem in high-dimensional systems.

2.1 Particle-based filtering methods

Filtering aims at estimating recursively the distribution $p(\mathbf{x}_{t_1:t_k} | \mathbf{y}_{t_1:t_k})$ (and in particular its marginal distribution $p(\mathbf{x}_{t_k} | \mathbf{y}_{t_1:t_k})$) at each observation time t_k . This filtering problem can be solved with a Monte Carlo sequential approach, called particle filtering (Del Moral et al., 2001; Doucet et al., 2000). The method relies on a Monte Carlo approximation of the filtering distribution over a set of weighted trajectories $\{\mathbf{x}_{t_1:t_k}^{(i)}\}_{i=1:N}$ (called particles):

$$\hat{p}(\mathbf{x}_{t_1:t_k} | \mathbf{y}_{t_1:t_k}) = \sum_{i=1}^N w_{t_k}^{(i)} \delta_{\mathbf{x}_{t_1:t_k}^{(i)}}(\mathbf{x}_{t_1:t_k}), \quad (3)$$

whose marginal distribution at time t_k writes:

$$\hat{p}(\mathbf{x}_{t_k} | \mathbf{y}_{t_1:t_k}) = \sum_{i=1}^N w_{t_k}^{(i)} \delta_{\mathbf{x}_{t_k}^{(i)}}(\mathbf{x}_{t_k}). \quad (4)$$

Particle filters rely on a sequential importance sampling scheme that recursively samples particles, and updates their weights at observation times. The weights corresponds to the ratio between the target distribution and the importance sampling distribution $\pi(\mathbf{x}_{t_k} | \mathbf{x}_{t_0:t_{k-1}}, \mathbf{y}_{t_1:t_k})$. They are recur-

125 sively computed as follows:

$$w_{t_k}^{(i)} \propto w_{t_{k-1}}^{(i)} \frac{p(\mathbf{y}_{t_k} | \mathbf{x}_{t_k}^{(i)}) p(\mathbf{x}_{t_k}^{(i)} | \mathbf{x}_{t_{k-1}}^{(i)})}{\pi(\mathbf{x}_{t_k}^{(i)} | \mathbf{x}_{t_0:t_{k-1}}^{(i)}, \mathbf{y}_{t_1:t_k})}. \quad (5)$$

In practice, a resampling procedure is added in order to avoid degeneracy. This procedure duplicates trajectories with large weights and remove small weighted trajectories.

2.1.1 Standard particle filter

130 When the proposal distribution π is set to the prior (i.e. $\pi(\mathbf{x}_{t_k} | \mathbf{x}_{t_0:t_{k-1}}, \mathbf{y}_{t_1:t_k}) = p(\mathbf{x}_{t_k} | \mathbf{x}_{t_{k-1}})$), the weights updating rule (5) simplifies to the computation of the data likelihood $p(\mathbf{y}_{t_k} | \mathbf{x}_{t_k}^{(i)})$. This particular instance of the particle filter is called the *Bootstrap filter* or sequential importance resampling (SIR) filter Gordon et al. (1993). Due to its simplicity it is the most commonly used particle filter. It is however a very inefficient distribution for high dimensional space as it does not take into account
135 the current observation and depends only weakly on the past data through the filtering distribution estimated at the previous instant. This distribution requires a great number of particles to explore meaningful areas of the state space.

2.1.2 Weighted Ensemble Kalman filter (WEnKF)

One way to efficiently incorporate observation within the proposal distribution consists to rely on
140 the ensemble Kalman filtering mechanism to define this distribution. This is the idea proposed in the WEnKF technique (Papadakis et al., 2010). In the WEnKF approach the importance sampling is taken as a Gaussian approximation of $p(\mathbf{x}_{t_k} | \mathbf{x}_{t_{k-1}}, \mathbf{y}_{t_k})$. This approach is close to the technique proposed in Van Leeuwen (2010). A variation of a similar technique based on a deterministic square-root formulation is also described in Beyou et al. (2013). In order to make the estimation of the
145 filtering distribution exact (up to the sampling), each member of the ensemble must be weighted at each observation instant t_k with appropriate weights $w_{t_k}^{(i)}$, defined from (5). Therefore, the Weighted ensemble Kalman filter (WEnKF) procedure can be simply summarized by Algorithm 1.

Algorithm 1 The WEnKF algorithm

For each $t_k = t_1, t_2, \dots$:

- Start from particles set $\{\mathbf{x}_{t_{k-1}}^{(i)}, i = 1, \dots, N\}$ and observation \mathbf{y}_{t_k}
 - Obtain particles set $\{\mathbf{x}_{t_k}^{(i)}, i = 1, \dots, N\}$ from:
 - **EnKF step:** Get $\mathbf{x}_{t_k}^{(i)}, i = 1, \dots, N$, from the assimilation of \mathbf{y}_{t_k} with an EnKF procedure;
 - **Computation of weights:** $w_{t_k}^{(i)} \propto w_{t_{k-1}}^{(i)} \frac{p(\mathbf{y}_{t_k} | \mathbf{x}_{t_k}^{(i)}) p(\mathbf{x}_{t_k}^{(i)} | \mathbf{x}_{t_{k-1}}^{(i)})}{p(\mathbf{x}_{t_k}^{(i)} | \mathbf{x}_{t_{k-1}}^{(i)}, \mathbf{y}_{t_k}^{(i)})}$;
 - **Resampling:** For $j = 1, \dots, N$, sample with replacement index $I(j)$ from discrete probability $\{w_{t_k}^{(i)}, i = 1, \dots, N\}$ over $\{1, \dots, N\}$ and set $\mathbf{x}_{t_k}^{(j)} = \mathbf{x}_{t_k}^{I(j)}$. Set $w_{t_k}^{(i)} = \frac{1}{N} \quad \forall i = 1, \dots, N$.
-

Note that particle-based filtering techniques update the filtering distribution at observation times only. However, after the estimate $\hat{p}(\mathbf{x}_{t_k} | \mathbf{y}_{t_1:t_k})$ has been updated at observation time t_k , the filtering distribution can be predicted in order to have a continuous estimation of $\hat{p}(\mathbf{x}_t | \mathbf{y}_{t_1:t_k})$ for all $t \in]t_k, t_{k+1}[$ until the next observation time:

$$\hat{p}(\mathbf{x}_t | \mathbf{y}_{t_1:t_k}) = \sum_{i=1}^N w_{t_k}^{(i)} \delta_{\mathbf{x}_t^{(i)}}(\mathbf{x}_t), \quad (6)$$

where, for all $i = 1, \dots, N$, the state $\mathbf{x}_t^{(i)}$ is sampled from (1), starting from $\mathbf{x}_{t_k}^{(i)}$.

155 2.2 Fixed-lag smoothing problem

Contrary to the filtering approach that uses past and present observations, the smoothing in state-space models aims at estimating $p(\mathbf{x}_t | \mathbf{y}_{t_1:t_{\text{end}}})$ for all $t \in [t_1, t_{\text{end}}]$, using all past and future observations over a given time period. As raised in the introduction, existing smoothing methods do not apply directly to a general non linear model of type (1) in a high-dimensional context, since assumptions have to be made that may not be realistic. Instead of solving the global smoothing, we will concentrate in the rest of the paper on a fixed-lag smoothing, which constitutes a partial answer to the global smoothing problem.

The objective of the fixed-lag smoothing will be to replace the predictive distribution (6) by its smoothed version $p(\mathbf{x}_t | \mathbf{y}_{t_1:t_{k+1}}) \forall t \in]t_k, t_{k+1}[$, sequentially each time a new observation $\mathbf{y}_{t_{k+1}}$ arrives. This will allow to reduce the temporal discontinuities inherent to the filtering technique, that successively predicts the distribution of the state between observations, and updates this distribution at observation times.

To achieve this, by construction of the particle filter that weights entire trajectories (see equation

(3)), it is known (see for instance Doucet et al. (2000)) that the fixed-lag smoothing distribution
 170 $\hat{p}(\mathbf{x}_t | \mathbf{y}_{t_1:t_{k+1}})$ can be directly obtained from the marginal at time t of $\hat{p}(\mathbf{x}_{t_1:t_{k+1}} | \mathbf{y}_{t_1:t_{k+1}})$. The
 empirical smoothing distribution is then given by:

$$\hat{p}(\mathbf{x}_t | \mathbf{y}_{t_1:t_{k+1}}) = \sum_{i=1}^N w_{t_{k+1}}^{(i)} \delta_{\mathbf{x}_t^{(i)}}(\mathbf{x}_t) \quad \forall t \in]t_k, t_{k+1}]. \quad (7)$$

However, this approximation is simply a reweighting of past existing particle trajectories, and relies
 on the support of the filtering distribution at time t_k . If the number of particles is too small with
 175 respect to the state dimension, the support may be greatly reduced by the correction step (assigning
 small weights to all particles except a few), leading in practice to a bad estimation of $p(\mathbf{x}_t | \mathbf{y}_{t_1:t_{k+1}})$.
 Moreover, if particle trajectories have been forced towards observations during the filtering step (like
 in the WEnKF procedure), a smoothing based on those particles will fail because it will not be able
 to correct discontinuities. Consequently, since we are interested in smoothing techniques that are
 180 efficient in a high-dimensional context, this direct smoothing technique can not be used in its basic
 form and has to be improved.

In the following, we propose to use a conditional simulation technique of diffusions that will
 enable the sampling of new smoothed trajectories between times t_k and t_{k+1} . The approximation of
 the smoothing distribution (7) at each hidden time will then be improved. The conditional simulation
 185 technique is presented in the next section, before the resulting smoothing procedure we propose.

3 Fixed-lag smoothing with conditional simulation

The smoothing method we propose is based on a conditional simulation technique that is presented in
 section 3.1. We develop then in section 3.2 how this technique can be used to improve the estimation
 of the smoothing distribution (7).

190 3.1 Conditional simulation

Conditional simulation of a diffusion aims at sampling trajectories from a given process:

$$d\mathbf{x}(t) = f(\mathbf{x}(t))dt + \sigma(\mathbf{x}(t))d\mathbf{B}(t) \quad (8)$$

between two times $t = 0$ and $t = T$, with the constraints $\mathbf{x}(0) = \mathbf{u}$ and $\mathbf{x}(T) = \mathbf{v}$. This simulation
 problem is treated by Delyon and Hu (2006), where the authors show how to obtain the law of
 195 the constrained process from a Girsanov theorem. In practice, the proposed algorithms consist in
 simulating trajectories according to another diffusion process, which is built to respect the constraints
 and is easy to simulate from. The conditional distribution of the constrained process (8) is absolutely
 continuous with respect to the distribution of the auxiliary process, with explicitly given density. For
 instance, in the case where the drift is bounded (a similar algorithm is proposed in Delyon and Hu
 200 (2006) for the unbounded case) and for σ invertible, the algorithm is based on the simulation of

trajectories from the following process:

$$d\tilde{\mathbf{x}}(t) = \left(f(\tilde{\mathbf{x}}(t)) - \frac{\tilde{\mathbf{x}}(t) - \mathbf{v}}{T-t} \right) dt + \sigma(\tilde{\mathbf{x}}(t)) d\mathbf{B}(t), \quad (9)$$

with initial condition $\tilde{\mathbf{x}}(0) = \mathbf{u}$. Note that Lemma 4 in Delyon and Hu (2006) deals with the existence of a unique solution for this equation. This process is a simple modification of (8), where a deterministic part is added to the drift. It is then easy to simulate unconditional trajectories from this process, and all simulated trajectories will satisfy $\tilde{\mathbf{x}}(T) = \mathbf{v}$ by construction. For simplicity we will assume in the following that σ is independent of $\mathbf{x}(t)$ (note however that this is not an assumption in Delyon and Hu (2006)). The law of the conditioned process is given by:

$$\mathbb{E}[h(\mathbf{x}) | \mathbf{x}(0) = \mathbf{u}, \mathbf{x}(T) = \mathbf{v}] = \mathbb{E}[h(\tilde{\mathbf{x}})\alpha(\tilde{\mathbf{x}})], \quad (10)$$

for all measurable function h , where:

$$\alpha(\tilde{\mathbf{x}}) = \exp \left(- \int_0^T \frac{(\tilde{\mathbf{x}}(t) - \mathbf{v})^T \Sigma^{-1} f(\tilde{\mathbf{x}}(t))}{T-t} dt \right) \quad (11)$$

is the density coming from Girsanov theorem (see Delyon and Hu (2006)), with $\Sigma = \sigma(\tilde{\mathbf{x}}(t))\sigma(\tilde{\mathbf{x}}(t))^T$.

Let us note that the presence of the drift part of model (8) in the auxiliary process (9) is crucial to make the simulation efficient. The same process had initially been proposed by Clark (1990) to solve the conditional simulation problem. On the other hand, standard Brownian bridges that could be used as auxiliary processes (Durham and Gallant, 2002) lead in practice to poor approximations of the original constrained diffusion in our high-dimensional setting, since Brownian bridge trajectories are too far away from trajectories of (8).

In the following, the conditional marginal of interest $p(\mathbf{x}_t | \mathbf{x}(0) = \mathbf{u}, \mathbf{x}(T) = \mathbf{v})$ will then be approximated as follows:

$$\hat{p}(\mathbf{x}_t | \mathbf{x}(0) = \mathbf{u}, \mathbf{x}(T) = \mathbf{v}) = \sum_{j=1}^M \alpha(\tilde{\mathbf{x}}^{(j)}) \delta_{\tilde{\mathbf{x}}_t^{(j)}}(\mathbf{x}_t) \quad \forall t \in [0, T], \quad (12)$$

where the M trajectories $\{\tilde{\mathbf{x}}_t^{(j)}\}_{j=1:M}$ are simulated from (9) with $\tilde{\mathbf{x}}_0^{(j)} = \mathbf{u}$ for all $j = 1, \dots, M$.

3.2 Proposed fixed-lag smoothing method

We show in the following how the conditional simulation technique can be used to improve the estimation of the local smoothing distribution $p(\mathbf{x}_t | \mathbf{y}_{t_1:t_{k+1}})$ for all $t \in [t_k, t_{k+1}]$.

We first note that this distribution can be decomposed as:

$$\begin{aligned} p(\mathbf{x}_t | \mathbf{y}_{t_1:t_{k+1}}) &= \int p(\mathbf{x}_t, \mathbf{x}_{t_k}, \mathbf{x}_{t_{k+1}} | \mathbf{y}_{t_1:t_{k+1}}) d\mathbf{x}_{t_k} d\mathbf{x}_{t_{k+1}} \\ &= \int p(\mathbf{x}_{t_k}, \mathbf{x}_{t_{k+1}} | \mathbf{y}_{t_1:t_{k+1}}) p(\mathbf{x}_t | \mathbf{x}_{t_k}, \mathbf{x}_{t_{k+1}}, \mathbf{y}_{t_1:t_{k+1}}) d\mathbf{x}_{t_k} d\mathbf{x}_{t_{k+1}}. \end{aligned} \quad (13)$$

Then, from the state-space model properties, we obtain:

$$230 \quad p(\mathbf{x}_t | \mathbf{y}_{t_1:t_{k+1}}) = \int p(\mathbf{x}_{t_k}, \mathbf{x}_{t_{k+1}} | \mathbf{y}_{t_1:t_{k+1}}) p(\mathbf{x}_t | \mathbf{x}_{t_k}, \mathbf{x}_{t_{k+1}}) d\mathbf{x}_{t_k} d\mathbf{x}_{t_{k+1}}. \quad (14)$$

Moreover, from the particle filter Monte Carlo approximation described by (3), the joint law $p(\mathbf{x}_{t_k}, \mathbf{x}_{t_{k+1}} | \mathbf{y}_{t_1:t_{k+1}})$ can be replaced by:

$$\hat{p}(\mathbf{x}_{t_k}, \mathbf{x}_{t_{k+1}} | \mathbf{y}_{t_1:t_{k+1}}) = \sum_{i=1}^N w_{t_{k+1}}^{(i)} \delta_{(\mathbf{x}_{t_{k+1}}^{(i)}, \mathbf{x}_{t_k}^{(i)})}(\mathbf{x}_{t_{k+1}}, \mathbf{x}_{t_k}), \quad (15)$$

where the $w_{t_{k+1}}^{(i)}$ are the particle filter importance weights.

235 Plugging (15) into (14) leads then to the following approximation for the fixed-lag smoothing distribution:

$$\hat{p}(\mathbf{x}_t | \mathbf{y}_{t_1:t_{k+1}}) = \sum_{i=1}^N w_{t_{k+1}}^{(i)} p(\mathbf{x}_t | \mathbf{x}_{t_k}^{(i)}, \mathbf{x}_{t_{k+1}}^{(i)}). \quad (16)$$

The conditional distribution $p(\mathbf{x}_t | \mathbf{x}_{t_k}^{(i)}, \mathbf{x}_{t_{k+1}}^{(i)})$ can be estimated using (12) for each pair of initial and end points $\mathbf{x}_{t_k}^{(i)}$ and $\mathbf{x}_{t_{k+1}}^{(i)}$:

$$240 \quad \hat{p}(\mathbf{x}_t | \mathbf{x}_{t_k}^{(i)}, \mathbf{x}_{t_{k+1}}^{(i)}) = \sum_{j=1}^M \alpha(\tilde{\mathbf{x}}_t^{(i)(j)}) \delta_{\tilde{\mathbf{x}}_t^{(i)(j)}}(\mathbf{x}_t), \quad (17)$$

where each $\tilde{\mathbf{x}}_t^{(i)(j)}$ is sampled from (9) with initial constraint $\tilde{\mathbf{x}}_{t_k}^{(i)(j)} = \mathbf{x}_{t_k}^{(i)}$ and final constraint $\tilde{\mathbf{x}}_{t_{k+1}}^{(i)(j)} = \mathbf{x}_{t_{k+1}}^{(i)}$.

The estimation of the smoothing distribution of interest writes finally:

$$\hat{p}(\mathbf{x}_t | \mathbf{y}_{t_1:t_{k+1}}) = \sum_{i=1}^N w_{t_{k+1}}^{(i)} \sum_{j=1}^M \alpha(\tilde{\mathbf{x}}_t^{(i)(j)}) \delta_{\tilde{\mathbf{x}}_t^{(i)(j)}}(\mathbf{x}_t), \quad \forall t \in]t_k, t_{k+1}]. \quad (18)$$

245 The algorithm we propose to compute the fixed-lag smoothing distribution on a given time interval $]t_k, t_{k+1}]$ is therefore the following:

Algorithm 2 Fixed-lag conditional smoothing

For each $t_k = t_1, t_2, \dots$:

- Store $\{\mathbf{x}_{t_k}^{(i)}\}_{i=1:N}$ and compute $\{\mathbf{x}_{t_{k+1}}^{(i)}\}_{i=1:N}$ and associated weights $\{w_{t_{k+1}}^{(i)}\}_{i=1:N}$ from a particle filter algorithm;
 - For each pair $\{\mathbf{x}_{t_k}^{(i)}, \mathbf{x}_{t_{k+1}}^{(i)}\}$, $i = 1, \dots, N$:
 - Simulate M conditional trajectories $\{\tilde{\mathbf{x}}_t^{(i)(j)}\}_{j=1:M}$ for $t \in [t_k, t_{k+1}]$ from (9) with an Euler scheme, with the constraints $\tilde{\mathbf{x}}_{t_k}^{(i)(j)} = \mathbf{x}_{t_k}^{(i)}$ and $\tilde{\mathbf{x}}_{t_{k+1}}^{(i)(j)} = \mathbf{x}_{t_{k+1}}^{(i)}$,
 - Compute weights $\alpha(\tilde{\mathbf{x}}_t^{(i)(j)})$ from (11) for all $j = 1, \dots, M$, with final constraint $\mathbf{x}_{t_{k+1}}^{(i)}$;
 - Compute $\hat{p}(\mathbf{x}_t | \mathbf{y}_{t_1:t_{k+1}}) = \sum_{i=1}^N w_{t_{k+1}}^{(i)} \sum_{j=1}^M \alpha(\tilde{\mathbf{x}}_t^{(i)(j)}) \delta_{\tilde{\mathbf{x}}_t^{(i)(j)}}(\mathbf{x}_t)$ for all $t \in]t_k, t_{k+1}]$.
-

4 One-dimensional simulation study

In this section, the smoothing method is first experimented on a one-dimensional state space model.

250 Since the proposed approach relies on a preliminary particle filtering step, filtering results are first presented in Section 4.2 (either considering a standard particle filter or the WEnKF). The results obtained with the standard fixed-lag smoothing method are then shown in Section 4.3. Finally, Section 4.4 presents the smoothing results obtained with the proposed technique.

4.1 State space model

255 The one-dimensional state space model of interest is a sine diffusion, partially observed with noise (used as an illustration by Fearnhead et al. (2008) for a particle filtering method) :

$$dx(t) = \sin(x(t))dt + \sigma_x dB(t), \tag{19}$$

$$y_{t_k} = x_{t_k} + \gamma_{t_k}, \tag{20}$$

where $\sigma_x^2 = 0.5$ and $\gamma_{t_k} \sim \mathcal{N}(0, \sigma_y)$ with $\sigma_y^2 = 0.01$. One trajectory of the process is first simulated
 260 from (19) with an Euler-type discretization scheme of time step $\Delta t = 0.005$. This trajectory will constitute the hidden process, observed through y_{t_k} generated according to (20) at every time step t_k , with $t_k - t_{k-1} = 20\Delta t$. The trajectory is plotted on Figure 1, together with the corresponding discrete observations at times t_k .

265

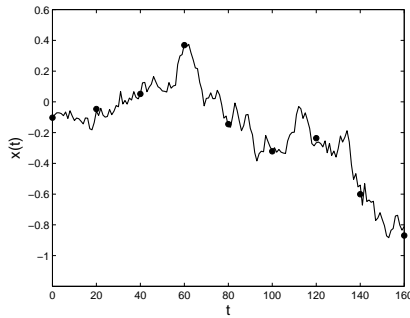


Fig. 1: Simulated sine diffusion trajectory $x(t)$ and partial observations $y(t_k)$ (dots) with $t_k - t_{k-1} = 20\Delta t$.

4.2 Particle filtering results

The filtering results are presented for the standard particle filter (denoted PF in the following) and the Weighted Ensemble Kalman filter (WEnKF). Two situations are shown, with reduced ($N = 20$) and high number ($N = 10000$) of particles. The case with a high number of particles is shown as
 270 the reference for comparison purpose, note however that this ideal situation is not reachable in a

high-dimensional context, since the number of particles has to be reduced for evident computational cost reasons.

The results for the two configurations are presented on Figure 2, where the dotted lines represents the filtering mean estimates. The filtering distribution $p(x_{t_k} | y_{t_1:t_k})$ is estimated at each observation time t_k using (4), and predicted between observation times from (6). The mean is then estimated from weighted particles as $\sum_{i=1}^N w_{t_k}^{(i)} x_t^{(i)}$, for all $t \in [t_k, t_{k+1}[$. Figure 2 (a)-(b) show that the standard particle filter results diverge from the reference solution between observation times, for low or high number of particles. As a matter of fact, when no observation is available, the state distribution is predicted from the dynamics only, so that particles trajectories are not guided towards the next observation. At observation times t_k , high weights are given to particles that are close to the observation, so that the estimated mean suddenly gets closer to the solution. These discontinuities between measurement times can also be observed on the WEnKF results (Figure 2 (c)-(d)), because particle trajectories are brutally corrected with the EnKF step at observation times. A smoothing will aim at reducing these temporal discontinuities while providing dynamically consistent solutions.

285

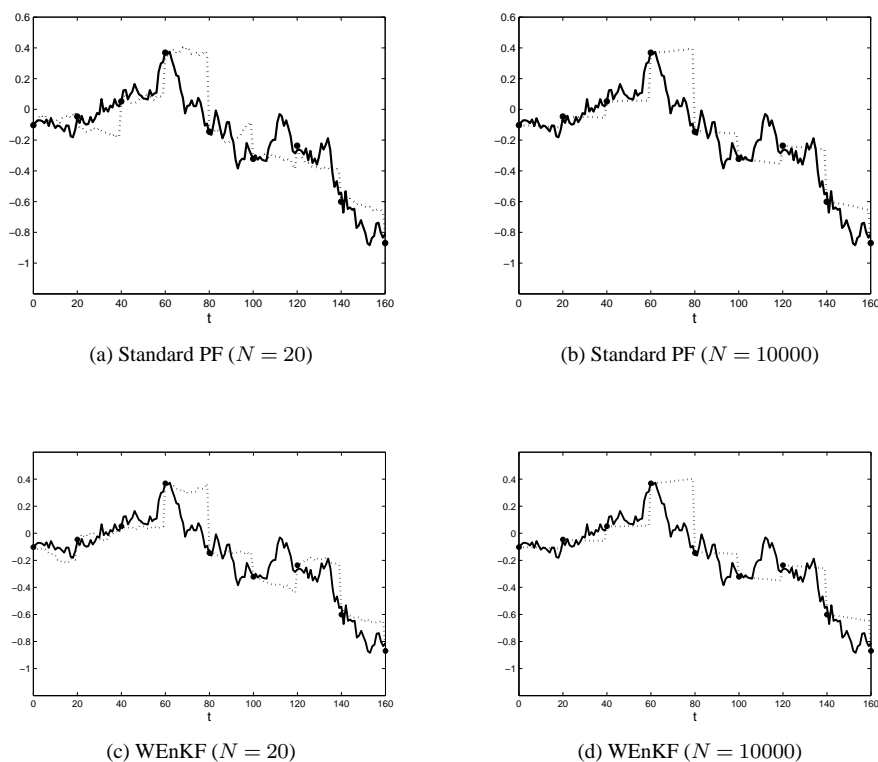


Fig. 2: Standard PF and WEnKF results. Thick line: hidden diffusion; Dots: partial observations; Dotted line: estimated filtering mean.

4.3 Standard fixed-lag smoothing results

From the particle filtering results, we present now the results obtained with the direct particles smoothing procedure described in section 2.2. This procedure relies on existing trajectories. The smoothing distribution $\hat{p}(x_t|y_{t_1:t_{k+1}})$ is computed backward for all $t \in]t_k, t_{k+1}]$ using expression (7), each time a new observation $y_{t_{k+1}}$ becomes available. The smoothing mean is computed as $\sum_{i=1}^N w_{t_{k+1}}^{(i)} x_t^{(i)}$ for all $t \in]t_k, t_{k+1}]$, and the standard deviation is computed in the same way from the weighted particles.

It can be observed on Figure 3(a) that the smoothing based on the standard particle filter is not efficient when the number of particles N is small: Only a few particles are close to the observation at time t_k and have nonzero weights, implying that the smoothing distribution is poorly estimated (see for instance between observation times $t = 100$ and $t = 120$ where the smoothing distribution is artificially peaked but far from the hidden trajectory). The smoothing result obtained from the reference configuration $N = 10000$ is plotted on Figure 3(b). In that situation, since many trajectories have high weights at observation times, the estimation of backward smoothing distributions is improved and includes the hidden trajectory.

Moreover, Figure 3(c)-(d) shows that the standard smoothing based on the WEnKF result fails for low or high number of particles. As a matter of fact, particle trajectories are artificially corrected by the EnKF step at each observation time. Resulting trajectories are highly non-plausible. Even for a huge number of particles, a smoothing based on those existing trajectories is not able to reduce the induced time discontinuities.

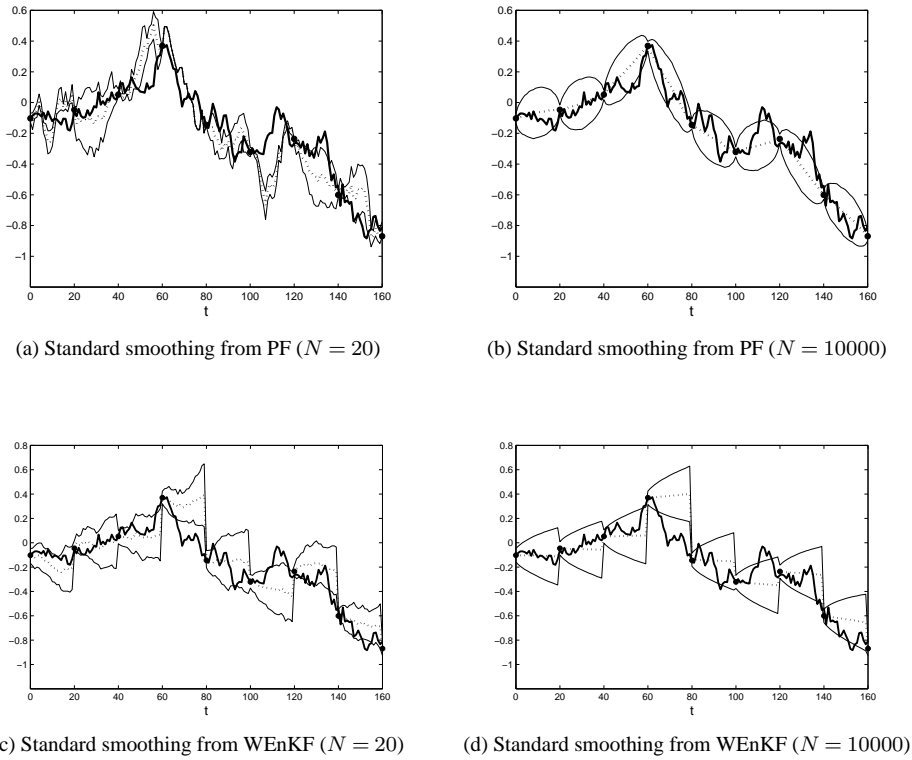


Fig. 3: Standard smoothing from PF and WEnKF results. Thick line: hidden diffusion; Dots: partial observations; Dotted line: estimated filtering mean.

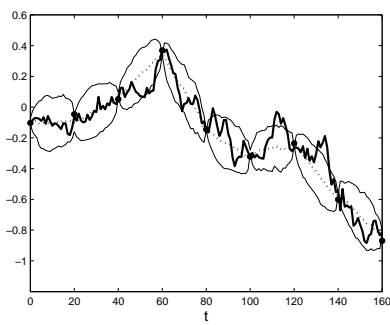
4.4 Proposed smoothing results

310 In this section, we show how the proposed method can improve the estimation of backward smoothing distributions when it is not adequate to rely on existing trajectories only. This is the case if the number of particles is too small, as demonstrated from the experiment presented on Figure 3(a), or if the existing trajectories do not correspond to plausible trajectories of the model (as shown for the WEnKF result on Figure 3(c)-(d)).

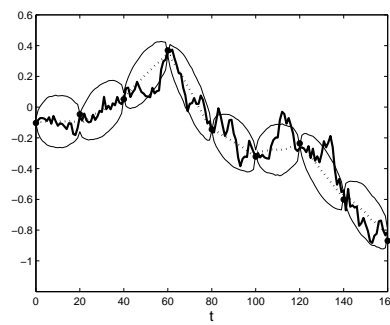
315 Our smoothing is first applied using the filtering output of the standard particle filter with $N = 20$ particles. Figure 4(a) shows the result obtained with a sampling of $M = 50$ conditional trajectories between each pair $\{x_{t_k}^{(i)}, x_{t_{k+1}}^{(i)}\}$, $i = 1, \dots, N$. The smoothing distribution $\hat{p}(x_t | y_{t_1:t_{k+1}})$ is computed from (18), so the smoothing mean is computed as $\sum_{i=1}^N w_{t_k}^{(i)} \sum_{j=1}^M \alpha(\tilde{x}^{(i)(j)}) \tilde{x}_t^{(i)(j)}$ for all $t \in]t_k, t_{k+1}]$, and similarly for the standard deviation. This result highlights the fact that since
 320 the proposed method creates new trajectories, it is able to correct the deficiencies of the standard smoothing approach presented on Figure 3(a) when the initial number of filtering particles is too small. On Figure 4(b), the same experiment is presented using $M = 500$ conditional trajectories. In that case, the result is very similar to the reference particles smoothing result presented on Figure 3(b), obtained from a particle filter with $N = 10000$.

325 In parallel, the proposed smoothing has been tested using the output of the WEnKF filtering
 technique with $N = 20$ particles. Again, the smoothing is computed with $M = 50$ and $M = 500$
 conditional trajectories, and the corresponding results are presented on Figure 3(c)-(d). Instead on
 relying on existing WEnKF trajectories that may not be plausible trajectories of the model (because
 of the EnKF correction step), the proposed method samples new trajectories between observation
 330 times. This leads to a good estimation of the smoothing distributions, contrary to the standard
 smoothing presented of Figure 3(c). Note that the smoothing results are very similar to the result
 obtained from the standard particle filter (Figure 3(a)-(b)) because both filters have similar behaviour
 at observation times.

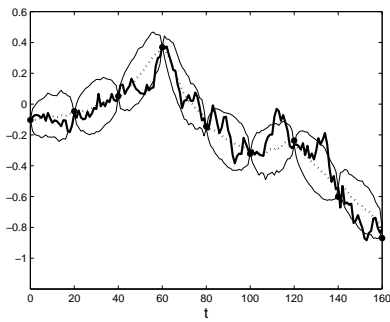
335



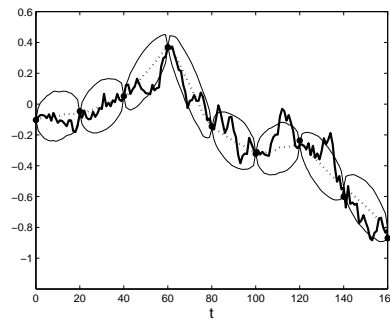
(a) Proposed smoothing from standard PF
 ($N = 20$ and $M = 50$)



(b) Proposed smoothing from standard PF
 ($N = 20$ and $M = 500$)



(c) Proposed smoothing from WEnKF
 ($N = 20$ and $M = 50$)



(d) Proposed smoothing from WEnKF
 ($N = 20$ and $M = 500$)

Fig. 4: Proposed conditional smoothing result. Thick line: hidden diffusion; Dots: partial observations; Dotted line: estimated backward smoothing mean; Thin line: estimated standard deviation.

5 Application to a high-dimensional assimilation problem

This section aims at illustrating the applicability of our method to a high-dimensional and non linear scenario, without extensive study at this stage. The method is applied to a turbulence assimilation problem, where the model of interest is of type (1). The goal is to recover temporal estimates of velocity/vorticity over a given spatial domain of size $n = 64 * 64$, from a sequence of noisy observations and a continuous *a priori* dynamical model based on a stochastic version of Navier-Stokes equation. Within an environmental framework, a direct application would be the estimation of wind fields or sea surface currents from satellite data.

5.1 State space model

Let $\xi(\mathbf{x})$ denote the scalar vorticity at point $\mathbf{x} = (x, y)^T$, associated to the 2D velocity $w(\mathbf{x}) = (w_x(\mathbf{x}), w_y(\mathbf{x}))^T$ through $\xi(\mathbf{x}) = \frac{\partial w_y}{\partial x} - \frac{\partial w_x}{\partial y}$. Let $\boldsymbol{\xi} \in \mathbb{R}^n$ be the state vector describing the vorticity over a $n = 64 * 64$ square domain, and $\mathbf{w} \in \mathbb{R}^{2n}$ the associated velocity field over the domain. We will focus on incompressible flows such that the divergence of the velocity field is null. A stochastic version of Navier-Stokes equation in its velocity-vorticity form can then be written as:

$$d\boldsymbol{\xi}_t = -\nabla \boldsymbol{\xi}_t \cdot \mathbf{w}_t dt + \frac{1}{Re} \Delta \boldsymbol{\xi}_t dt + \sigma d\mathbf{B}_t, \quad (21)$$

where \Re denotes the flow Reynolds number ($Re = 3000$). The uncertainty is modeled by a Brownian motion of size n , with covariance $\Sigma = \sigma \sigma^T$, where $\sigma \in \mathbb{R}^n$. A velocity field example, generated from the model (21), is shown on Figure 5(a), together with the corresponding vorticity map (b).

We assume the hidden vorticity vector $\boldsymbol{\xi}$ is observed through noisy measurements \mathbf{y}_{t_k} at discrete times t_k , where $t_k - t_{k-1} = 100\Delta t$, and $\Delta t = 0.1$ is the time step used to discretize (21). In our experimental setup, measurements correspond to PIV (Particle Image Velocimetry) image sequences used in fluid mechanics applications. Note however that other kind of data can be used similarly within this state space model, like meteorological or oceanographic data for instance. The state and observation are related in our case through $\mathbf{y}_{t_k} = g(\boldsymbol{\xi}_{t_k}) + \gamma_{t_k}$, where g is a non linear function linking the vorticity to the image data, and γ_{t_k} is a Gaussian noise, uncorrelated in time.

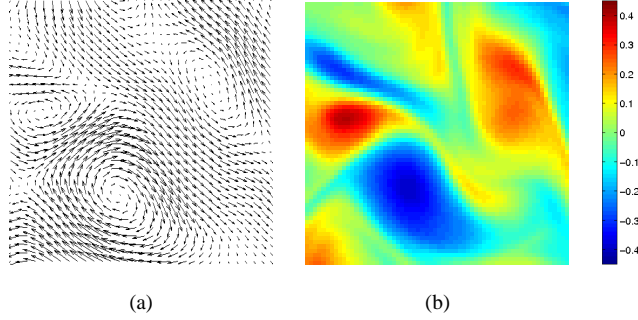


Fig. 5: State example. (a) Velocity field w_t ; (b) Associated vorticity map ξ_t .

5.2 Implementation details

We recall that the smoothing relies first on a particle filter step. Due to the high dimensionality of the state vector, the use of a standard particle filter is not adapted to solve the filtering problem, as discussed by Snyder et al. (2008) or Van Leeuwen (2009). We make then use of the method presented by Papadakis et al. (2010) which combines the benefits of the ensemble Kalman filter, known to perform well in practice for high dimensional systems (Stroud et al., 2010), and the particle filter (which solves theoretically the true filtering problem, without approximating the filtering distributions with Gaussian distributions). Since the method of Papadakis et al. (2010) is intrinsically a particle filter, it leads then at each observation time t_k to a set of particles and weights $\{\xi_{t_1:t_k}^{(i)}, w_{t_k}\}_{i=1:N}$, as required by the algorithm proposed in section 3.

The particle filter step requires simulations from the dynamical model (21), and the conditional simulation step requires to sample trajectories from its constrained version, which consists in a similar problem with modified drift (see process (9)). The model is discretized in time with time step $\Delta t = 0.1$; more information about the discretization scheme may be obtained in Papadakis et al. (2010). The random perturbations are assumed to be realizations of Gaussian random fields that are correlated in space with Gaussian covariance function $\Sigma(\mathbf{x}_i, \mathbf{x}_j) = \eta \exp(-\frac{\|\mathbf{x}_i - \mathbf{x}_j\|^2}{\lambda})$, where $\eta = 0.01$ and $\lambda = 13$. In practice, the simulation of these perturbations is performed in Fourier space, with the method described in Evensen (2003).

Finally, the estimation of the smoothing distributions require the computation of conditional trajectories weights, corresponding to Girsanov weights given by (11). After a Riemann sum approximation of the integral, the computation of weights requires the inversion of the matrix Σ of size (n, n) , where $n = 64 * 64$ is the number of grid points. We choose to compute Σ^{-1} empirically using a singular value decomposition computed from the M realizations of the perturbation fields used for the constrained trajectories simulations. Let \mathbf{Z} be the matrix of size (n, M) containing the M centered fields of size $n = 64 * 64$, the SVD leads to $\mathbf{Z} = \mathbf{U}\mathbf{D}\mathbf{V}^T$, so that $\mathbf{Z}\mathbf{Z}^T = \mathbf{U}\mathbf{D}\mathbf{D}^T\mathbf{U}^T$. The inverse of the covariance matrix Σ^{-1} is finally computed as:

$$M(\mathbf{Z}\mathbf{Z}^T)^{-1} = M\mathbf{U}(\mathbf{D}\mathbf{D}^T)^{-1}\mathbf{U}^T, \quad (22)$$

390 which only requires the inversion of a diagonal. Note that more efficient procedures could be imple-
 mented in our case (homogeneous Gaussian covariance) since the covariance function is separable in
 x and y directions. This means that the covariance matrix Σ can be written as the Kronecker product
 of smaller matrices and more easily inverted (Sun et al., 2012). However, the SVD inversion can be
 applied to any covariance structure, in particular it could deal with a non homogeneous covariance
 395 matrix.

5.3 Results

In this section, we illustrate the capability of the proposed method to reduce the temporal disconti-
 nuities inherently introduced by the filtering in continuous-discrete state-space models.

The smoothing result relies on the output of the WEnKF filtering step, computed with $N = 500$
 400 particles. Compared to the size of the system, the number of particles is theoretically too small for
 the filter to be truly efficient. In practice, many filtering trajectories have close to zero weights at
 observation times. Histograms of filtering weights are given as illustration on Figure 6(a)-(b) at two
 times $t = 400$ and $t = 500$. Note however that the filter is not degenerate and is able to provide
 results that get close to the hidden vorticity at measurement times. This can be observed on Figure 7,
 405 where the mean square error is plotted with full line, averaged at each time over the image domain
 of size $n = 64 * 64$. Since the ground truth vorticity sequence is known in our experimental setup,
 the mean square error is computed between the hidden vorticity and the estimated filtering mean,
 given by $\sum_{i=1}^N w_{t_k}^{(i)} \xi_t^{(i)}$ for all $t \in [t_k, t_{k+1}[$. The correction steps lead to successive error decreases
 at observation times.

410 The proposed smoothing method has been applied with $M = 200$. Note that we take benefit
 from the fact that many filtering trajectories have close to zero weights. Indeed, the smoothing method relies
 in practice on a reduced number $\tilde{N}M$ of sampled conditional trajectories (with $\tilde{N} \ll N$), which
 makes the problem computationally tractable. On this experiment, we have retained around 5%
 of initial filtering trajectories. The smoothing distribution $\hat{p}(\xi_t | \mathbf{y}_{t_1:t_{k+1}})$ is computed for all $t \in$
 415 $[t_k, t_{k+1}]$ from (18), and its mean is computed as $\sum_{i=1}^N w_{t_{k+1}}^{(i)} \sum_{j=1}^M \alpha(\tilde{\xi}^{(i)(j)}) \tilde{\xi}_t^{(i)(j)}$. Histograms
 of conditional simulation weights $\alpha(\tilde{\xi}^{(i)(j)})$ are given as illustration on Figure 6(c)-(d) for a given
 particle (i) at two times $t = 400$ and $t = 500$.

The mean square error is computed between the true vorticity and the estimated smoothing mean,
 and plotted on Figure 7 with dotted line. As expected, the smoothing method reduces the error at
 420 hidden times between observations.

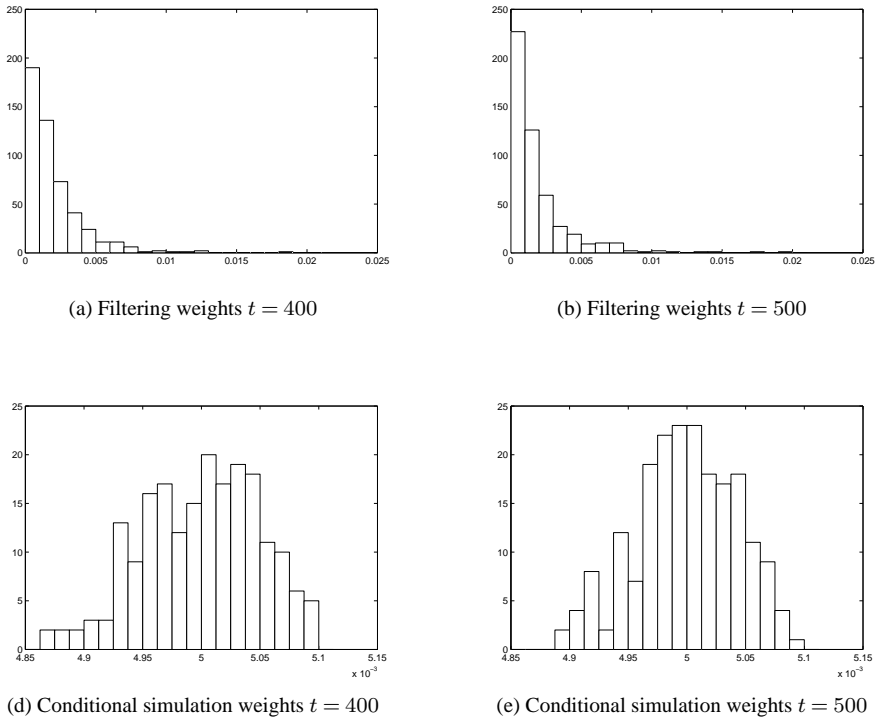


Fig. 6: Filtering and conditional simulation weights

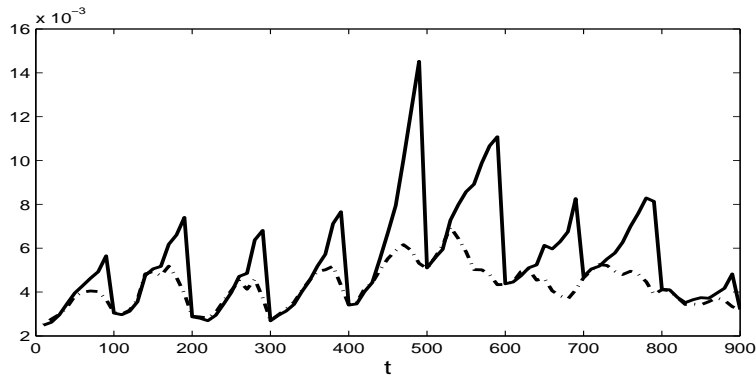


Fig. 7: Full line: mean square error between ground truth vorticity and estimated filtering mean; Dotted line: mean square error between ground truth vorticity and estimated backward smoothing mean.

425 In addition, we present below a qualitative evaluation of the smoothing result for the same experiment, over a specific time interval.

The WEnKF result is first presented on Figure 8 for the time interval $[400, 500]$ between two observations, where estimated mean vorticity maps are computed as $\sum_{i=1}^N w_{400}^{(i)} \xi_t^{(i)}$ for all $t \in [400, 500[$,

and as $\sum_{i=1}^N w_{500}^{(i)} \xi_t^{(i)}$ for $t = 500$. The temporal discontinuity between estimations can be observed
430 when reaching observation time $t = 500$: the vorticity map is suddenly modified in order to fit to
the observations, introducing inconsistencies in the vorticity temporal trajectories. Note that the ap-
plication of the standard particles smoothing (described in section 2.2) will fail here, and not only
because the number of particles is too small. As a matter of fact, we recall that the filtering trajec-
435 tories have been computed from the method presented in Papadakis et al. (2010), which uses the
ensemble Kalman filter step as importance distribution in the particle filter algorithm. The ensemble
Kalman filter consists of a prediction step from the dynamical model (21), and a correction step
which shifts particles towards the observation. Because of this correction step, the sampled filter-
ing trajectories between two observation times do not correspond to trajectories of the dynamical
440 model. This implies that from such a particle filter, the standard smoothing based on existing tra-
jectories will not be able to reduce the temporal discontinuities observed on Figure 8. This can be
observed on Figure 9, where smoothed vorticity maps are computed as $\sum_{i=1}^N w_{400}^{(i)} \xi_t^{(i)}$ for $t = 400$,
and as $\sum_{i=1}^N w_{500}^{(i)} \xi_t^{(i)}$ for all $t \in]400, 500]$. The discontinuity at time $t = 500$ is still present.

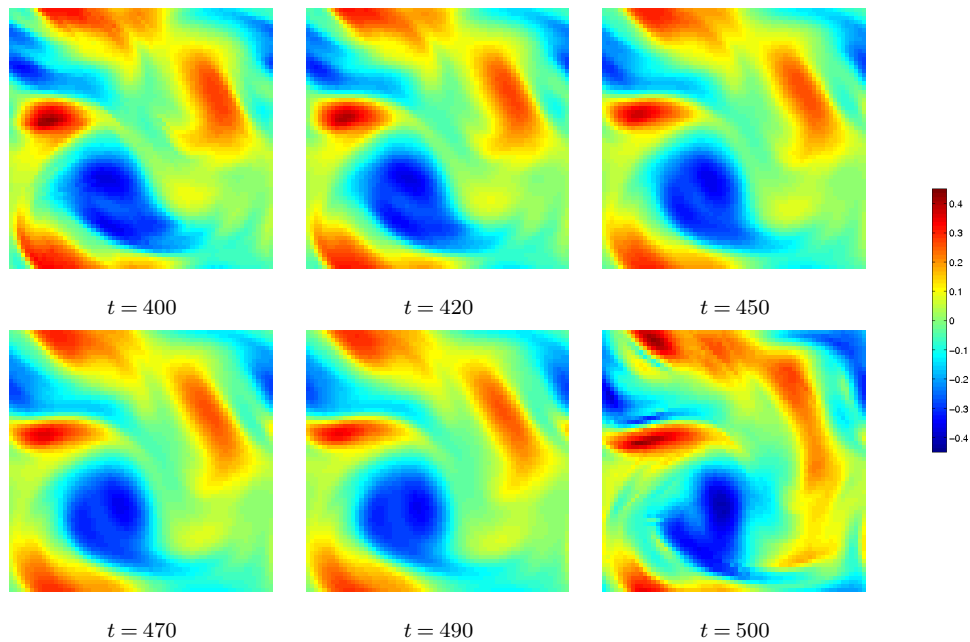


Fig. 8: Filtering result with the method of Papadakis et al. (2010). Estimated mean vorticity maps for different
times t between observation times $t = 400$ and $t = 500$.

445

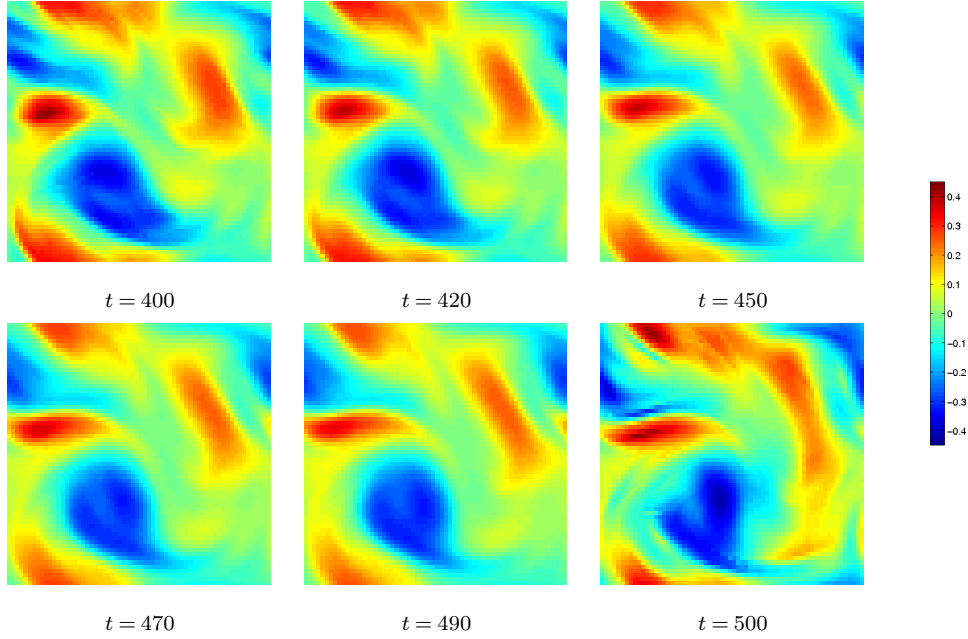


Fig. 9: Standard particles smoothing result (see Section 2.2). Estimated mean vorticity maps for different times t between observation times $t = 400$ and $t = 500$.

The result obtained with the proposed method is plotted on Figure 10. Estimated mean vorticity maps are computed as $\sum_{i=1}^N w_{500}^{(i)} \sum_{j=1}^M \alpha(\tilde{\xi}^{(i)(j)}) \tilde{\xi}_t^{(i)(j)}$ for all $t \in [400, 500]$. Spatio-temporal vorticity trajectories are gradually modified until observation time $t = 500$, preserving the fluid flow properties. As a matter of fact, since the proposed method samples new trajectories from the law of the physical process (21), the smoothed vorticity trajectories are by construction consistent with the *a priori* dynamical model. In order to sample the smoothed trajectories, the method relies on the model and on filtering marginals at observation times, but not on filtering trajectories at hidden times. It is then able to smooth the discontinuities inherent to the particle filtering technique we have used, contrary to the standard smoothing presented on Figure 9.

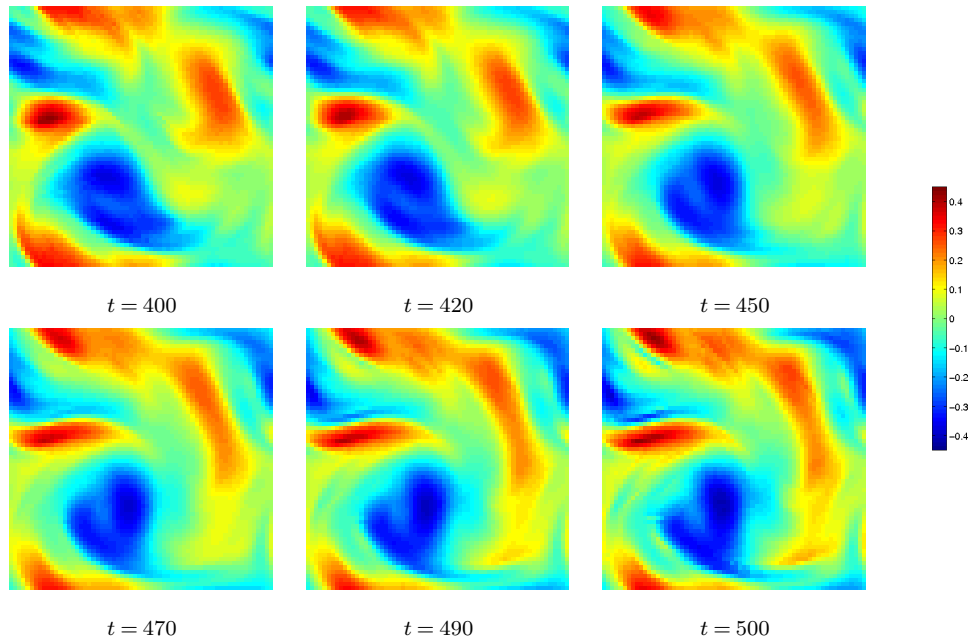


Fig. 10: Smoothing result with the proposed method. Estimated mean vorticity maps for different times t between observation times $t = 400$ and $t = 500$.

6 Conclusion and discussion

In this paper we introduced a smoothing algorithm based on a conditional simulation technique of
460 diffusions. The proposed smoothing is formulated as fixed-lag, in the sense that it is performed
sequentially each time a new observation appears, in order to correct the state at hidden times up to
the previous observation. Note that a decomposition similar to equations (13) to (18) can be written
from an integration up to a previous time t_{k-h} , with $h > 1$. This implies that the smoother can be
formulated with a larger fixed-lag, in order to correct the state backward not only up to the previous
465 observation, but up to further measurement times. Yet, due to the successive resampling steps that
have been performed in the filtering steps before time t_k , there are in practice only a few distinct
filtering trajectories at times t_{k-h} if h is large. Consequently, the estimation of the joint law in (15)
will not be reliable anymore for a too large value of h .

We have shown the practical applicability of the method to a high-dimensional problem. Never-
470 theless, the algorithm remains costly since a second Monte Carlo step is added to the Monte Carlo
nature of particle filter algorithms. Yet, from an algorithmic point of view, the sequential nature of
the proposed technique allows the smoothing to be implemented with a similar structure as filtering
methods (sequential sampling and weighting of model trajectories). It is then easy to couple this
smoothing to an operational filtering system and benefit from parallelization strategies for instance.

475 Since the proposed smoothing uses the filtering result as input, it relies on the success of the

underlying particle filter. For high-dimensional systems, a standard particle filter is not adapted and it is necessary to use filtering techniques that guide particles towards observations. In this paper, we use the WEnKF algorithm. In practice, any efficient particle filtering technique with such a guiding can be used within our framework. Note however that the construction of such techniques remains
480 an open area of research.

We plan to work on the application of the smoothing method to a real high-dimensional case (for the estimation of sea surface currents from satellite image sequences). However, such a work will imply numerous difficulties which are not related to the smoothing technique but to the definition of the state-space model: definition of a suitable physical model, good characterization of state noise
485 structure and model parameters. Therefore, this will be part of a future work.

References

- Beskos, A. and Roberts, G. O.: Exact simulation of diffusions, *The Annals of Applied Probability*, 15, 2422–2444, 2005.
- 490 Beskos, A., Papaspiliopoulos, O., Roberts, G. O., and Fearnhead, P.: Exact and computationally efficient likelihood-based estimation for discretely observed diffusion processes (with discussion), *Journal of the Royal Statistical Society: Series B*, 68, 333–382, 2006.
- Beyou, S., Cuzol, A., Gorthi, S., and Mémin, E.: Weighted Ensemble Transform Kalman Filter for Image Assimilation, *TellusA*, 65, 2013.
- Briers, M., Doucet, A., and Maskell, S.: Smoothing algorithms for state-space models, *Annals of the Institute of Statistical Mathematics*, 62, 61–89, 2010.
- 495 Clark, J.: The simulation of pinned diffusions, in: *Proceedings of the 29th IEEE Conference on Decision and Control*, pp. 1418–1420, 1990.
- Del Moral, P.: *Feynman-Kac Formulae. Genealogical and Interacting Particle Systems with Applications*, Springer, 2004.
- 500 Del Moral, P., Jacod, J., and Protter, P.: The Monte Carlo Method for filtering with discrete-time observations, *Probability Theory and Related Fields*, 120, 346–368, 2001.
- Delyon, B. and Hu, Y.: Simulation of conditioned diffusions and applications to parameter estimation, *Stochastic Processes and Applications*, 116, 1660–1675, 2006.
- Doucet, A., Godsill, S., and Andrieu, C.: On sequential Monte Carlo sampling methods for Bayesian filtering, *Statistics and Computing*, 10, 197–208, 2000.
- 505 Durham, G. and Gallant, A.: Numerical techniques for maximum likelihood estimation of continuous-time diffusion processes, *Journal of Business and Economic Statistics*, 20, 297–316, 2002.
- Evensen, G.: The ensemble Kalman filter: theoretical formulation and practical implementation, *Ocean dynamics*, 53, 343–367, 2003.
- 510 Evensen, G. and van Leeuwen, P.: An ensemble Kalman Smoother for nonlinear dynamics, *Monthly Weather Review*, 128, 1852–1867, 2000.
- Fearnhead, P., Papaspiliopoulos, O., and Roberts, G.: Particle filters for partially observed diffusions, *Journal of the Royal Statistical Society B*, 70, 755–777, 2008.
- Godsill, S. J., Doucet, A., and West, M.: Monte Carlo smoothing for nonlinear time series, *Journal of the American Statistical Association*, 99, 156–168, 2004.
- 515 Gordon, N., Salmond, D., and Smith, A.: Novel approach to non-linear/non-Gaussian Bayesian state estimation, *IEEE Processing-F*, 140, 1993.
- Papadakis, N., Mémin, E., Cuzol, A., and Gengembre, N.: Data assimilation with the weighted ensemble Kalman filter, *Tellus Series A: Dynamic Meteorology and Oceanography*, 62, 673–697, 2010.
- 520 Snyder, C., Bengtsson, T., Bickel, P., and Anderson, J.: Obstacles to high-dimensional particle filtering, *Monthly Weather Review*, 136, 4629–4640, 2008.
- Stroud, J. R., Stein, M. L., Lesht, B. M., Schwab, D. J., and Beletsky, D.: An ensemble Kalman filter and smoother for satellite data assimilation, *Journal of the American Statistical Association*, 105, 978–990, 2010.
- Sun, Y., Bo, L., and Genton, M. G.: Geostatistics for large datasets, in: *Advances and challenges in space-time modelling of natural events*, pp. 55–77, Springer, 2012.
- 525

Van Leeuwen, P. J.: Particle filtering in Geophysical systems, *Monthly Weather Review*, 137, 4089–4114, 2009.

Van Leeuwen, P. J.: Nonlinear data assimilation in geosciences: an extremely efficient particle filter, *Quarterly Journal of the Royal Meteorological Society*, 136, 1991–1999, 2010.

Van Leeuwen, P. J. and Ades, M.: Efficient fully nonlinear data assimilation for geophysical fluid dynamics, *Computers and Geosciences*, 55, 16–27, 2013.